

Avoided Band Crossing in Locally Periodic Elastic Rods

R. A. Méndez-Sánchez,* A. Morales, and J. Flores†

Centro de Ciencias Físicas UNAM, P. O. Box 48-3, 62251 Cuernavaca, Morelos, México

Avoided band crossings have been studied theoretically and it has been shown that they can provide a tuning of the metal-insulator transition. Here we present an experimental example of an avoided band crossing for a classical undulatory system: torsional waves in locally periodic rods. To excite and detect the torsional waves, an electromagnetic-acoustic transducer for low-frequencies that we have recently developed, is used. Calculations performed using the transfer matrix method agree with the experimental measurements. In the observed avoided band crossing one level, which is a border-induced bulk level, moves from one band to the next.

PACS numbers: 43.20.+g, 71.20.-b, 46.40.-f, 62.30.+d

In a seminal paper, Wigner and von Neumann [1] studied the repulsion of the discrete energy levels of quantum systems when an external parameter ϵ is varied. For states of the same symmetry they obtained what is called avoided level crossing [2]. In general, however, the spectrum of a quantum system is not of the discrete type. For instance, periodic systems show a band spectrum with extended wave amplitudes according to Bloch's theorem. If the coupling between these bands is neglected we arrive to one-band models, such as the Anderson [3] or the Harper models [4, 5]. When an external parameter is varied in these systems, some of the bands move up in energy and others move down, giving rise to band crossings. At these values of the parameter, however, the coupling among bands can no longer be neglected. This coupling gives rise to avoided band crossing (ABC), which is a generalization of the avoided level crossing mentioned above.

The ABC has been recently studied theoretically in the context of the kicked Harper model [6] and some unexpected results were found. The ABCs can provide a tuning of the metal-insulator transition and changes in the localization lengths, among other properties.

Although the ABCs have been studied in quantum-mechanical systems, they can also be obtained for classical undulatory systems such as electromagnetic, elastic or acoustic systems. Since we have recently dealt with elastic waves in rods with locally periodic structures, where wave amplitudes were measured and a band structure emerges [7], we are now able to study ABC in elastic vibrations. It is the purpose of this letter to show experimentally for the first time the existence of an ABC. Besides their intrinsic interest, the results presented here are relevant for vibration isolation [8] and in the design of very narrow passband filters [9]. They could also be of importance in applications of acousto-optic fiber devices [10] and in the design of many aerospace and marine vehicles [11].

The rods of finite length L analyzed here consist of N identical unit cells of length l , as shown in Fig. 1. Each cell is formed by three cylinders, one of length $l - \epsilon$, radius R and cross section area S , and two cylinders of length $\epsilon/2$, radius r and cross section area s . In this way

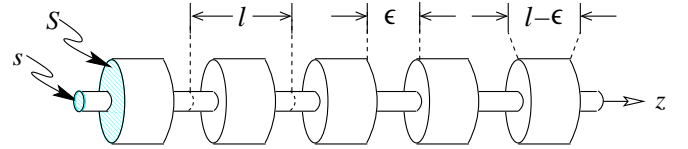


FIG. 1: Geometry of the rod. The length of the unit cell is l and ϵ is the width of the notch. Here S and s are the cross section areas of the rod and notches, respectively.

a rod with N obstacles is formed and ϵ is the external parameter to be varied. We assume $R \ll L$ and $R \ll \lambda = 2\pi/k$, where λ is the normal-mode wavelength, so the system behaves indeed as one dimensional. Torsional waves in this rod then obey the wave equation with a phase velocity $\sqrt{G/\rho}$, where G is the shear modulus and ρ is the density. The normal-mode spectrum of the rod is pure point but, as N increases, a band structure emerges [7].

A diagram of the experimental setup is given in Fig. 2. The signal of an oscillator (Stanford Research Systems,

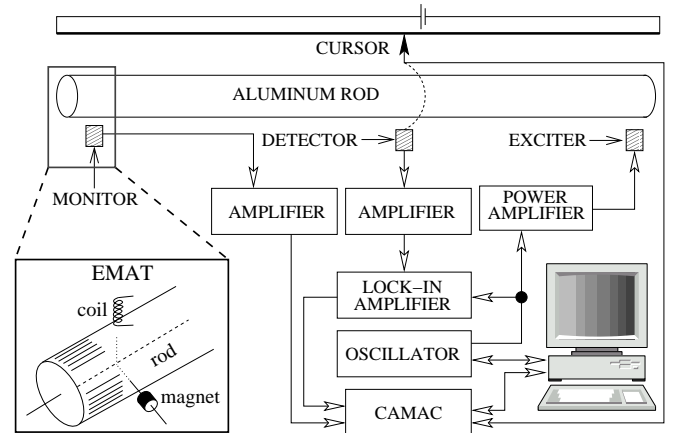


FIG. 2: Block diagram of the experimental setup. The EMATs (exciter, detector and monitor) are shown shaded. The dotted line indicates mechanical contact between the cursor (filled arrow) and the scanning detector. The schematic diagram of the EMAT is shown in the left lower corner.

Function Generator DS345) is sent to a power amplifier (Krhon-Hite 7500) and then to the electromagnetic-acoustic transducer (EMAT) exciter. This EMAT, as well as the one used as detector, consists of a coil and a magnet as shown in the left lower corner of Fig. 2. They are configured to excite or detect torsional waves without any mechanical contact with the rod. The signal from the EMAT scanning detector is amplified by a high-impedance amplifier. To monitor the resonances the signal is sent to the lock-in amplifier (EG&G PARC 128A). The latter converts the AC signal to a DC voltage, which is digitized by a CAMAC, whose output is sent to a PC. The DC voltage is proportional to the wave amplitude when exciting a normal mode of the rod. The reference signal for the lock-in was taken from the oscillator. The position z of the scanning detector along the rod axis is measured by mechanically coupling it to a cursor in contact with a nichrome wire, depicted by the bold line of Fig. 2. The signal of the voltage divider is then sent to the CAMAC and finally to the PC. The scanning detector as well as the cursor are moved with a motor (not shown) controlled by the PC and the CAMAC. The normal-mode wave amplitudes are then scanned along the rod. We should remark, however, that the resonant frequencies depend on temperature. Instead of controlling the latter, we changed the frequency of the exciter to follow the resonance. To do this, a third EMAT (denoted MONITOR in Fig. 2) is used to maintain the phase of the wave constant. The change in frequency is typically of the order of 0.1%, which is therefore the experimental error in the frequency measurements.

The theoretical normal-mode frequencies and their corresponding wave amplitudes were computed using the transfer matrix method [7]. In order to do this, we express the wave amplitude ψ_i in cylinder i as

$$\psi_i(z) = A_i e^{ik(z-z_{i-1})} + B_i e^{-ik(z-z_{i-1})}, \quad (1)$$

where $z_{i-1} \leq z \leq z_i$, $i = 1, 2, \dots, 2N+1$, and impose the following approximate boundary conditions at the points z_i , where the radius changes:

$$\psi_i|_{z_i} = \psi_{i+1}|_{z_i}; \quad s_i^2 \frac{\partial \psi_i}{\partial z} \Big|_{z_i} = s_{i+1}^2 \frac{\partial \psi_{i+1}}{\partial z} \Big|_{z_i}. \quad (2)$$

Here s_i equals either S or s according to the value of i . We shall consider the case of free ends, so Neumann boundary conditions hold at $z_0 = 0$ or $z_{2N+1} = L$. More details on the transfer matrix method for torsional waves in rods can be found in Ref. [7].

The spectra of the rods depend on ϵ/l , ϵ being the external parameter. When $\epsilon/l \neq 0, 1$ a band structure appears and the bands move up or down as ϵ/l varies. The coupling of the bands then leads to avoided band crossings. A typical ABC is shown in Fig. 3 for the second and third bands. The experimental results for $\epsilon/l = 0.4, 0.5$ and 0.6 correspond to the diamonds in the same figure. A good agreement is obtained between theory and

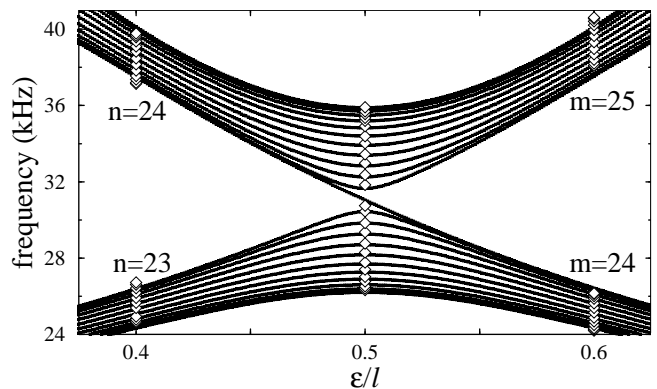


FIG. 3: Resonant frequencies as a function of ϵ/l for a locally periodic aluminum bar with $L = 120.0$ cm, $R = 6.45 \pm 0.05$ mm, $r = 3.2 \pm 0.05$ mm, and $N = 12$. The experimental values (diamonds) fit rather well with the numerical ones (continuous lines). The c -level corresponds to $n = m = 24$ nodes.

experiment. This is remarkable since no fitting parameter was used. Also, from the same figure it is possible to see that one level, which we shall call c , moves from one band to the other as the ABC takes place. We will discuss the nature of this level below.

In Fig. 4 we present some experimental wave amplitudes with number of nodes $n = 21, \dots, 27$ for $\epsilon/l = 0.4$ and $m = 21, \dots, 27$ for $\epsilon/l = 0.6$; they belong to the second and third bands, respectively. These are the wave amplitudes at the left- and right-hand side of the ABC, which occurs at $\epsilon/l = 0.5$, and correspond to the normal mode frequencies (diamonds) of Fig. 3. The results calculated with the transfer matrix method are given in Fig. 5. A nice agreement with the experimental wave amplitudes is obtained once we take into account the fact that at the position of the notches the detector lies farther away than when it is located above the cylinders of radius R . In our case, the experimental signal is reduced by a factor of the order of 8, so the theoretical values at the notches were divided by this factor.

As observed in these figures each wave amplitude in the second band is interchanged with one belonging to the third band located symmetrically in frequency with respect to the c -level, which corresponds to $n = 24$ in Figs. 4 and 5. For example, the wave amplitude for $\epsilon/l = 0.4$ and $n = 22$ is very similar to that with $m = 26$ for $\epsilon/l = 0.6$. They are, however, different because they do not have the same number of nodes. But the differences are negligible since they occur at points where the envelope of the wave amplitudes is negligible and a node bifurcates into three nodes.

To quantify how much the experimental wave amplitudes of the left-hand side of Fig. 4 mix with those at the right-hand side of the same figure, we plot in Fig. 6a the

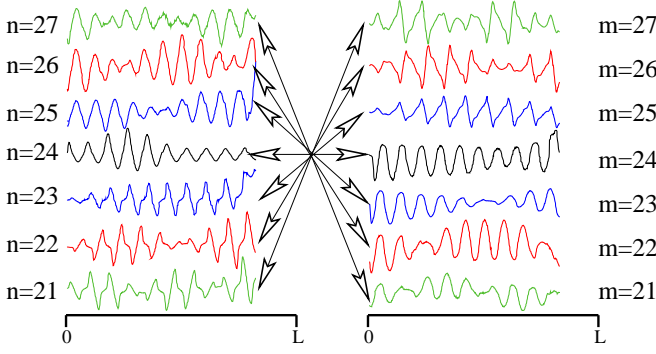


FIG. 4: Experimental torsional wave amplitudes (in arbitrary units) for an aluminum rod with $\epsilon/l = 0.4$ (left column) and $\epsilon/l = 0.6$ (right column). The amplitudes are not measured at the right-hand end of the rod since the signal obtained with the scanning detector is distorted by the exciter.

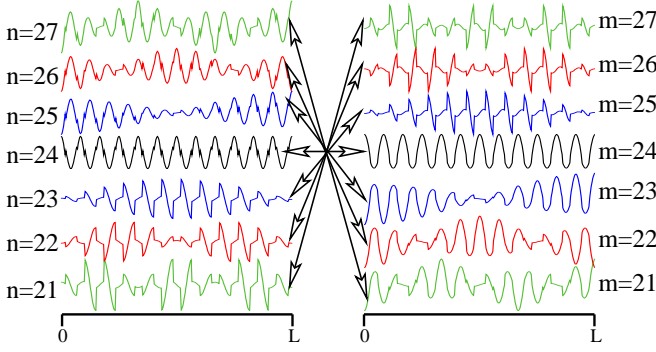


FIG. 5: Torsional wave amplitudes belonging to the second and third bands obtained with the transfer matrix method. The normal modes for $\epsilon/l = 0.4, 0.6$ (left and right columns) are labeled by $n = 21, \dots, 27$ and $m = 21, \dots, 27$, respectively.

absolute value of the overlap

$$\mathcal{O}_{nm} = \left| \int_0^L dz \psi^n(z; \epsilon/l = 0.4) \psi^m(z; \epsilon/l = 0.6) \right| \quad (3)$$

between the amplitudes $\psi^n(\epsilon/l = 0.4)$ and $\psi^m(\epsilon/l = 0.6)$ with $n, m = 21, \dots, 27$. The overlap is larger for wave functions that are symmetrical with respect to the c -level while it is negligible for other levels within the two bands involved in the ABC. This yields an anti-diagonal overlap matrix. The theoretical overlaps corresponding to the same wave amplitudes are given in Fig. 6b. Thus, experiment and theory agree very well and the overlap between theoretical and experimental wavefunctions is always larger than 0.84. These anti-diagonal correlations only appear when an ABC is present. To show this, in Fig. 6c we present a numerical calculation of \mathcal{O}_{nm} for wave amplitudes at $\epsilon/l = 0.4$ and $\epsilon/l = 0.45$, since in this range of ϵ/l no ABC is present. The overlap matrix is now concentrated along the diagonal since the wave amplitudes remain in its position within the band.

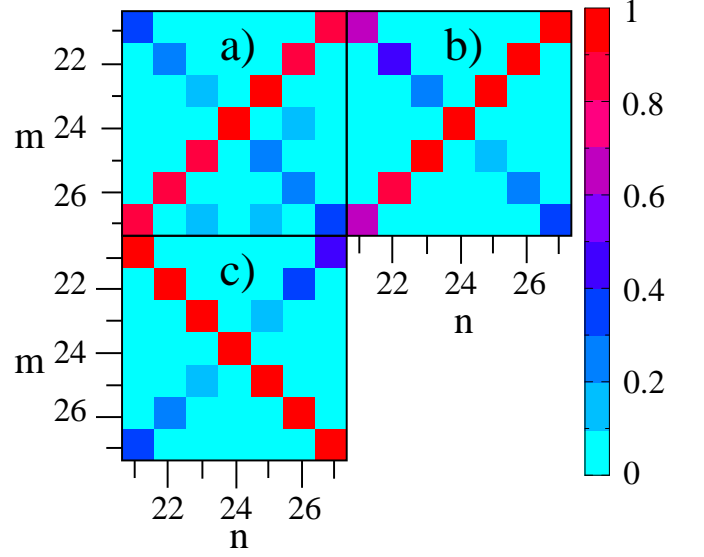


FIG. 6: Overlap \mathcal{O}_{nm} between wave amplitudes at $\epsilon/l = 0.4$ and $\epsilon/l = 0.6$; a) experimental results, b) numerical results. In c) is shown the overlap between theoretical wave amplitudes at $\epsilon/l = 0.35$ and $\epsilon/l = 0.4$.

So what is the nature of the c -level? It cannot be a Bloch-type state since at the ABC this level moves from one band to a neighboring one. Its existence must therefore be due to the fact that the system is finite so level c is really a border state. To corroborate this we

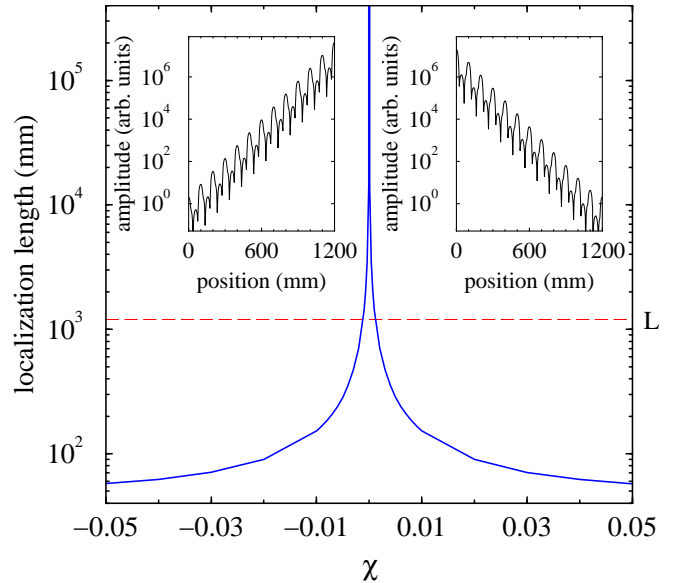


FIG. 7: Localization length of wavefunction $n = 24$ as a function of χ for $\epsilon/l = 0.4$. The dashed line indicates the length L of the rod. The insets at the left and right upper corners show the wave amplitudes for $\chi = -0.03$ and $\chi = 0.03$, respectively.

made the following transformation: $z_i \rightarrow z_i + \chi\epsilon/2$, with $i = 1, \dots, 2N$, which alters the two cylinders at the extremes, the system remaining otherwise locally periodic. The c -level is then localized. The localization length as a function of χ is given in Fig. 7. We see that when $\chi = 0$, the case corresponding to Figs. 4 and 5, the localization length is much larger than L , so the c -level appears to be an extended state, such as the one labeled $n = m = 24$. The c -level is actually a border-induced bulk state [12].

In conclusion, we have measured for the first time an avoided band crossing, in this case for torsional vibrations of elastic rods. Since we deal with a finite rod a level shifts from a given band to the next one. This state is an example of a border-induced bulk mode, as predicted in Ref. [12]. We have obtained a similar behavior for compressional waves and it is also expected for light and microwaves [13, 14].

We thank A. Díaz-de-Anda and A. Pimentel for their help in the experimental measurements. We also thank L. Gutiérrez, G. Báez and J. Maytorena for useful discussions and L. Mochán for a careful reading of the manuscript. This work was supported by DGAPA-UNAM project IN104400.

[†] Permanent address: Instituto de Física, UNAM, P. O. Box 20-364, 01000 México, D. F. México

- [1] J. von Neumann and E. P. Wigner, Z. Phys. **30**, 467 (1929).
- [2] L. D. Landau and E. M. Lifshitz, *Quantum Mechanics*, (Pergamon, Oxford, 1976), p. 304.
- [3] P. W. Anderson, Phys. Rev. **109**, 1492 (1958).
- [4] R. Peierls, Z. Phys. **80**, 763 (1933).
- [5] P. G. Harper, Proc. Phys. Soc. London A **68**, 874 (1955); M. Ya. Azbel, Sov. Phys. JETP **19**, 634 (1964); D. R. Hofstadter, Phys. Rev. B **14**, 2239 (1976); S. Aubry and G. André, Ann. Israel Phys. Soc. **3**, 133 (1980).
- [6] R. Ketzmerick, K. Kruse and T. Geisel, Phys. Rev. Lett. **80**, 137 (1998); L. Hufnagel et al, Phys. Rev. B **62**, 15348 (2000); R. Ketzmerick, K. Kruse, D. Springsguth, and T. Geisel, Phys. Rev. Lett. **84** 2929 (2000).
- [7] A. Morales, J. Flores, L. Gutiérrez, and R. A. Méndez-Sánchez, J. Acous. Soc. Am. **112**, 1961 (2002).
- [8] J. C. Snowdon, J. Acoust. Soc. Am. **66**, 1245 (1979).
- [9] J. C. Chen et al, J. Lightwave Technol. **14**, 2575 (1996).
- [10] A. Diez, G. Kakarantzas, T. A. Birks, and P. St. J. Russell Appl. Phys. Lett. **76**, 3481 (2000).
- [11] M. H. Marcus, B. H. Houston, and D. M. Photiadis, J. Acous. Soc. Am. **109**, 865 (2001).
- [12] D. Olguin and R. Baquero, Phys. Rev. B **50**, 1980 (1995); **51**, 16891 (1995).
- [13] C. Dembowski et al, Phys. Rev. E **60**, 3942 (1999).
- [14] U. Kuhl and H.-J. Stöckmann, Phys. Rev. Lett. **80**, 3232 (1998).

* Author to whom correspondence should be addressed;
Electronic address: mendez@fis.unam.mx